

NPS ARCHIVE  
1967  
KERR, W.

William A          Kerr

AN INVESTIGATION OF A PORTABLE DEVICE  
FOR DETERMINING  
LATERAL LOADS ON A HOLLOW CYLINDER.

Thesis  
K3893



AN INVESTIGATION OF A PORTABLE DEVICE FOR DETERMINING LATERAL  
LOADS ON A HOLLOW CYLINDER

by

LCDE. WILLIAM A. KERR, JR., U.S.N.

B.S., UNITED STATES NAVAL ACADEMY

(1957)

SUBMITTED IN PARTIAL FULFILLMENT

OF THE REQUIREMENTS FOR THE

DEGREE OF NAVAL ENGINEER

and

FOR THE DEGREE OF MASTER OF SCIENCE

IN NAVAL ARCHITECTURE

and

MARINE ENGINEERING

at the

MASSACHUSETTS INSTITUTE OF TECHNOLOGY

May, 1967

1965 ARCHIVE

Thesis - K 3893

1967

KERIC, W.

ABSTRACT

An Investigation of a Portable Device for Determining  
Lateral Loads on a Hollow Cylinder  
LCDR. William A. Terry, USN

Submitted to the Department of Naval Architecture and  
Marine Engineering on May 19, 1967 in partial fulfillment  
of the requirements for the degree of Naval Engineer  
and the Master of Science degree in Naval Architecture  
and Marine Engineering.

The object of the research was to investigate the  
feasibility of designing a portable device that would  
determine the force transmitted perpendicular to the axis  
of a hollow cylinder. An example of a hollow cylinder sub-  
jected to such a force system is an axle.

The method of investigation was analytical and con-  
centrated in the general conceptual region of utilizing  
the theory of elasticity to determine measurable quantities  
that occurred as direct result of the applied force system.  
In order to limit the scope and number of variations in-  
volved, the measurable quantity selected was the strain  
produced in a component of the measuring device by varia-  
tions in the slope parallel to the axis of the hollow  
cylinder resulting from the applied force system.

The analytical investigation showed that construction of  
a portable force-measuring device that depends on varying  
elastic curve to produce a measurable strain was impractical  
when the strain measurement was performed with an electrical  
resistance strain gage.

It is recommended that further investigation be con-  
ducted in the area of other changes in the geometry of the  
hollow-cylinder, a means of magnifying the changes in geometry  
and a means of remotely detecting very small displacements.

Thesis Supervisor: Dr. William M. Murray





TABLE OF CONTENTS

	<u>Page</u>
List of Symbols-----	4
Introduction-----	5
Analysis and Design-----	8
Result-----	22
Discussion of Results-----	23
Conclusions and Recommendations-----	24
Appendix-----	25
I. Manderla-Winkler Equations-----	26
II. Saint Venants' Principle-----	28
III. Curved Bars-----	32
IV. Sample Problem-----	39
Bibliography-----	41





# LIST OF SYMBOLS

$M$	-----bending moment
$a, l, L$	-----length
$E$	-----Youngs' Modulus of Elasticity
$I$	-----moment of inertia
$\tau$	-----slope of tangent to elastic curve
$\sigma$	-----stress
$\epsilon$	-----strain
$t$	-----thickness
$R$	-----average radius
$F, P$	-----concentrated forces
$\delta$	-----displacement
$h$	-----height
$e$	-----strain gage voltage drop



## 1. INTRODUCTION

The purpose of this thesis was to analytically design a portable device that would measure the force on a hollow cylinder acting as a beam.

The particular application that was used as a "vehicle" for design development was the design of a device that would determine the load on the axle of a cargo aircraft as it sits on the ground.

A cargo aircraft very often will be utilized on a route on which there are several stops. At each stop the plane loads, and unloads cargo, shifts cargo, and possibly refuels or shifts fuel. All these operations cause the weight and center of gravity to vary from their values when the plane is in the light condition. The value of weight and the location of the center of gravity are of vital importance to the pilot of the plane since they help to determine the take-off run required, the lift-off speed required, and the in-flight controllability and stability.

The portable device would enable the pilot to have a cockpit presentation of the force on each axle of the



aircraft. A simple calculation would then give him the information; or, an electrical circuit could be designed to combine the signals from the axles in such a way that aircraft weight and center of gravity would be presented directly. The present method of determining weight and center of gravity movement is to have a crewman calculate the change based on the estimated weight of cargo and its estimated distance from the location of the center of gravity of the empty aircraft. The method is very subject to human error and carelessness.

The desire for the device to be portable was motivated by two ideas. The first was that a company operating cargo aircraft would require only a few sets of the devices since they could be removed from aircraft not engaged in the multi-stop cargo hauling. The second reason was so that any user of the device would not require specifically trained personnel to install and remove the devices. (Portable has been used in the sense that the device is easily installed.)

The motivation for selecting the cargo aircraft as a "vehicle" of design development arose from interest of commercial agencies in obtaining a portable load measuring device, and a need to know the order of magnitude



of the forces and dimensions involved in analyzing the hollow cylinder and designing a device to measure its loading. However, there are many other uses to which such a device could be placed. With only a couple of pipes and a system of the portable devices, weighing stations could be quickly set up by untrained personnel. Such weighing stations would allow operators of conventional ships, container ships, and roll-on, roll-off cargo ships to ascertain cargo loads regardless of the sophistication or development of the port.





### ANALYSIS AND DESIGN

Examination of hollow cylinders supporting concentrated loads, such as aircraft axles, revealed that several structural models are applicable. The models considered were hollow cylinders acting as a simple beam with a concentrated load at mid-span, a fixed end beam with concentrated load at mid-span, and as a cantilevered beam with a concentrated load at the free end. In some cases the concentrated load represented the weight of the aircraft as it was transmitted down the strut, in some cases the concentrated load represented the ground reaction transmitted through the wheels. In any event, a model involving a concentrated load and some sort of support could be developed for any system of cargo aircraft landing gear arrangements, or, for any portable weighing station that might be proposed.

Since the objective was to design a portable device, it was decided to measure some deformation that would occur in the hollow cylinder. To this end the simple beam was analyzed in an attempt to discover a relation between the concentrated load and a deformation that could be detected. Figure I. shows the beam and its' associated shear and bending moment diagrams.



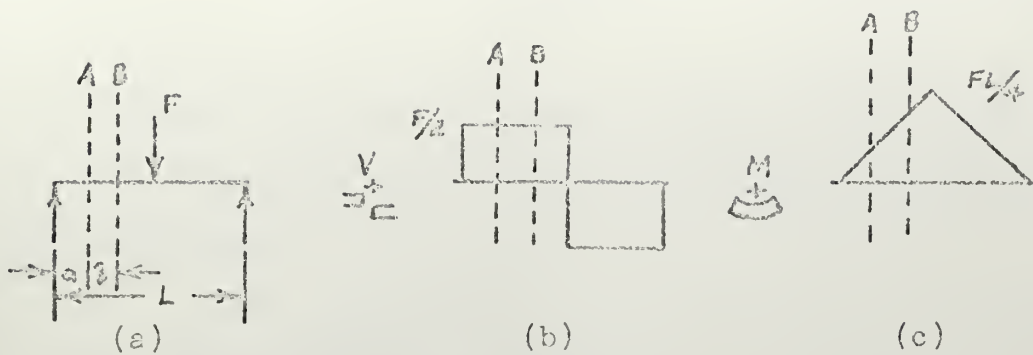


FIGURE I

(a) Simple Beam (b) Shear Diagram (c) Moment Diagram.

A section, A-B, of the beam was isolated. The moment on the A end of the section was determined to be

$$M_{AB} = \frac{F}{2} a \quad (1)$$

and on the B end of the section it was

$$M_{BA} = -\frac{F}{2} (a+b). \quad (2)$$

The sign convention used in equations (1) and (2) was that moments were considered positive when acting clockwise on the end of a section.

The moments on the ends of section A-B can also be determined from the Manderla-Winkler Equations which gave<sup>1</sup>.

$$M_{AB} = \frac{2EI}{l} (2\tau_a + \tau_b) \quad (3)$$

and

$$M_{BA} = \frac{2EI}{l} (\tau_a + 2\tau_b). \quad (4)$$

---

1. See Appendix I. for equation development. Note that  $\tau$  is the slope of the elastic curve and is positive when measured clockwise from the chord connecting the ends of the segment of beam.



Substitutions of Equations (1) and (2) into (3) and (4) yielded equations (5) and (6). Solving the latter two equations,

$$\frac{F}{2}a = \frac{2EI}{l}(2\tau_a + \tau_b) \quad (5)$$

$$-\frac{F}{2}a - \frac{F}{2}l = \frac{2EI}{l}(\tau_a + 2\tau_b) \quad (6)$$

to eliminate the dimension "a", led to a relation for F, equation (7), in terms of the elastic curve of the member.

$$F = \frac{12EI}{l^2}(\tau_a + \tau_b) \quad (7)$$

Similar analysis of a cantilevered beam yielded equation (8). Note that in both equations (7) and (8) that the magnitude of the concentrated load has been found to be proportional to the algebraic sum of the slope of the elastic curves at the end of the sections.

$$F = \frac{6EI}{l^2}(\tau_a + \tau_b) \quad (8)$$

The constants of proportionality are functions of the material of the structural member and the distance separating the ends of the arbitrary section A-B. It should also be noted that equations (7) and (8) are subject to the same limitations as the Manderla-Winkler Equations; principally that there can be no discontinuities in the  $M/EI$  curve within the span of "l."





Hereafter, the proportionality constant will be called  $C_1$ , and equation (9) represents all relations of concentrated load and elastic curve slope.

$$F = C_1 (\tau_2 + \tau_3) \quad (9)$$

With equation (9) in mind, the next step was to devise some way of determining the slope of the member from which the load that was causing the slope could be developed.

At this point it was assumed that simple beam theory would apply to the hollow cylinder. The Manderle-Winkler equations required that consideration be given only to a section with constant shear which confined any section such as A-B of Figure I, to an unloaded portion of the cylinder. Additionally, by suitably limiting the distance, " $l$ ", between ends of the segment under consideration and calling upon St. Venant's Principle,<sup>1</sup> it was possible to stay out of a region of complex local deformations. Based on the foregoing it was reasonable to assume that a segment of hollow cylinder could be selected that deformed elastically as a simple beam; that plane sections remained plane and that the radius of the cylinder remained constant.

---

1. See Appendix II.



It was decided to investigate the possibility of having some sort of arm maintained perpendicular to a surface of the cylinder which would have its tip deflected as the slope of the elastic curve varied. This deflection would cause a strain in another member which could in turn be measured by commercially available strain gages. This concept called for holding the perpendicular arms in position with some sort of spring loading within the case of the device and anchoring one end of the second, or strained member, to the case.

The member supporting the strain gage should be very flexible compared to the upright. Therefore, several types of thin curved bars were examined. Flexibility was desired so that the tip deflection of the arm and the slope of the elastic curve of the hollow cylinder would not be unduly distorted by resistance to deflection of the free end of the strained member.

The first thin curved bar examined was in the form of a one-half circle as shown in Figure II where P is a force exerted on the free end due to the deflection of the tip of the arm held perpendicular to the cylinder surface. Utilizing the equations of APPENDIX III, a relation can be developed between the free end deflection and a maximum strain. The relation for the case depicted in Figure II was as follows:





Figure 11

$\frac{1}{2}$  Circle Curved Bar

$$M = Px \quad (10)$$

$$x = R \sin \theta, \quad y = R(1 - \cos \theta), \quad ds = R d\theta \quad (11)$$

$$\delta_y = \int \frac{Mx}{EI} ds \quad (12)$$

$$\delta_z = \int \frac{My}{EI} ds \quad (13)$$

After substituting equations (10) and (11) into (12) and (13) the displacements toward the center of curvature,  $\delta_y$ , and perpendicular to the aforementioned,  $\delta_z$ , were found to be:

$$\delta_y = \frac{\pi}{2} \frac{PR^3}{EI} \quad (14)$$

$$\delta_z = 2 \frac{PR^3}{EI} \quad (15)$$

Then, since the curved bar is thin, a linear bending stress distribution was assumed across "t" which has a maximum value at  $\theta = \pi/2$ . In addition to the stress due to bending, making a free-body diagram of the half ring from  $\theta = \pi/2$  to the free end showed a force equal to P exerted normal to the cross section at  $\theta = \pi/2$ . The stresses that are



isted in the top and bottom fibers were

$$\sigma_{top} = -\frac{P}{A} + \frac{PRt}{2I} \quad (16)$$

$$\sigma_{bottom} = -\frac{P}{A} - \frac{PRt}{2I} \quad (17)$$

where the negative sign indicated fibers in compression for the loading depicted in Figure II. Equations (16) and (17) are cases of simple tension and, or, compression; therefore, a simple linear relation of stress and strain was utilized to relate the stress in the top and bottom fibers to the strains in those fibers.

$$\sigma = E \epsilon \quad (18)$$

$$\epsilon_{top} = \frac{1}{E} \left[ -\frac{P}{A} + \frac{PRt}{2I} \right] \quad (19)$$

$$\epsilon_{bottom} = \frac{1}{E} \left[ -\frac{P}{A} - \frac{PRt}{2I} \right] \quad (20)$$

And then by subtracting (20) from (19) the result was equation (21).

$$\epsilon = \epsilon_{top} - \epsilon_{bottom} = \frac{PRt}{EI} \quad (21)$$

This was readily solved for PR/EI and related to the free end deflections of the half ring. Similar analysis was made of the quarter and three quarter rings sketched in Figure III and the results are indicated by equations (22) where D is a constant with values shown in equation (23).





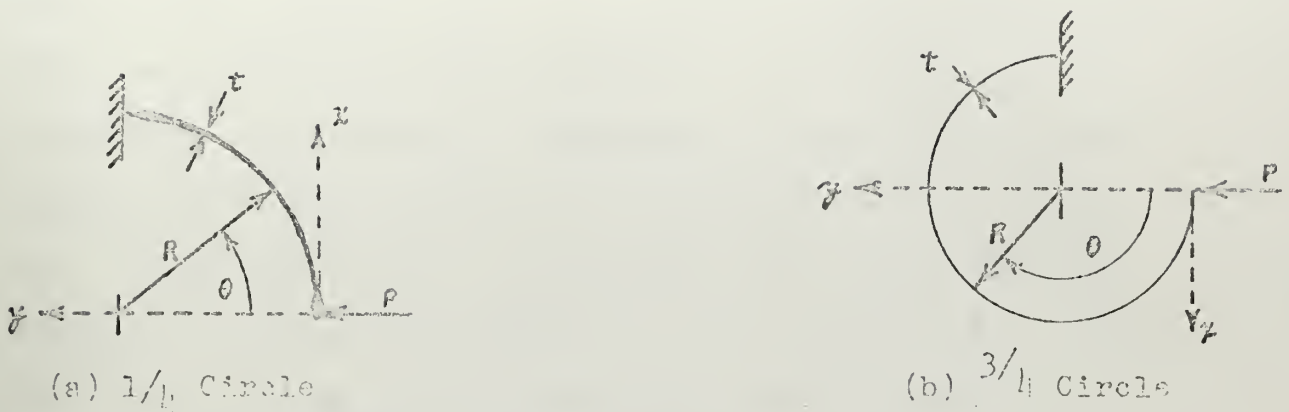


Figure III  
PARTIAL CURVED BARS

$$\delta_y = D \frac{R^2}{2} \epsilon = D \frac{PR^3}{EI} \quad (22)$$

$$D = \begin{cases} \frac{1}{4} \pi & - \frac{1}{4} \text{ circle} \\ \frac{1}{2} \pi & - \frac{1}{2} \text{ circle} \\ \frac{3}{4} \pi & - \frac{3}{4} \text{ circle} \end{cases} \quad (23)$$

The next step undertaken was to relate the tip deflection of the upright to the deflection of the free end of the various partial-circle curved bars and in turn relate the slope of the elastic curve of the hollow cylinder to the strain in the curved bar. As the slope changed, the tip of the upright would deflect. Assuming small slope variations, this deflection of the upright tip was given by equation (24) where  $h$  denotes the length of the upright.

$$\delta_{UPRIGHT} = \delta_o = h\tau \quad (24)$$



However, the upright tip is in contact with the curved bar. The pure displacement of the tip due to cylinder slope is reduced by an interactive displacement resulting from the upright tip being deflected as a cantilever by the curved bar. In addition, due to the upright and the curved bar being in contact, the deflection of the upright,  $\delta_u$ , equals the deflection,  $\delta_r$ , of the curved bar; and the force, P, causing the curved bar to deflect is equal to the force causing the interactive displacement of the upright tip.

$$\delta_u = h\tau - \delta_{\text{INTERACTION}} \quad (25)$$

$$\delta_r = \delta_u = h\tau - \delta_{\text{INT}} \quad (26)$$

$$\tau = \frac{1}{h} [\delta_r + \delta_{\text{INT}}] \quad (27)$$

Equation (27) was solved for P and equated to the force, expressed in terms of displacement, acting on the free end of a cantilever. This led to an expression, equation (28), for interactive displacement in terms of curved-bar free end displacement. In equation (28), and hereafter, the subscript u refers to the upright, subscript r refers to the curved bar.

$$\delta_{\text{INT}} = \frac{1}{30} \cdot \frac{h^3}{R^3} \cdot \frac{E_r I_r}{E_u I_u} \cdot \delta_r \quad (28)$$

By substitution of equation (28) into (27) an expression for slope in terms of curved bar displacement is obtained, equation (29).



$$h\tau = \left[ 1 + \frac{h^3}{30R^3} \cdot \frac{E_f I_f}{E_s I_s} \right] \delta_y \quad (29)$$

Equation (29) was then modified with equation (22) to finally arrive at an expression for slope in terms of strain, equation (30).

$$\tau = \left[ D \frac{R^2}{2h} + \frac{1}{3} \cdot \frac{h^2}{R^2} \cdot \frac{E_f I_f}{E_s I_s} \right] \epsilon \quad (30)$$

The slope was proportional to the algebraic sum of the top and bottom fiber strains. The constant of proportionality, which I called  $C_2$ , is a function of the geometry and material of the components of the measuring device. Equation (30) could thus be re-written as:

$$\tau = C_2 \epsilon \quad (31)$$

Now that relation had been developed between the concentrated loading on the hollow cylinder and the strain in the fibers of a flexural member, it was desired to select a particular type of curved bar; either in the form of a one-half circle or a three quarter circle. The idea of a quarter circle was discarded because of the location of the occurrence of maximum strain. It would occur at the first end of the quarter circle bar; a position where the placement of a strain gage would be impossible, and where the actual





strain differs from the theoretical by a large percentage. In other words, for a given hollow cylinder under a given loading it was desirable to utilize the type of curved bar that would result in the most sensitivity; that is to say, the bar that would produce the highest strain. This was accomplished by computing the constants,  $C_2$ , for each type of curved bar based on the geometry considerations and assumptions depicted in Figure IV.

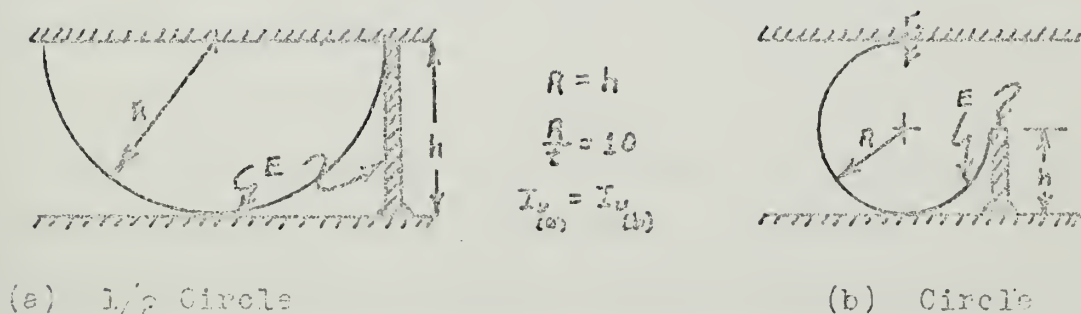


Figure IV.

#### Geometrical Assumptions for Evaluating $C_2$

From equations (30) and (23) and based on Figure IV, an expression for the relationship was developed which is given by equation (32)

$$\frac{\epsilon_{3/4 \text{ circle}}}{\epsilon_{1/2 \text{ circle}}} = \frac{C_2 \text{ 1/2 circle}}{C_2 \text{ 3/4 circle}} \quad (32)$$

$$\frac{\epsilon_{3/4}}{\epsilon_{1/2}} = \frac{\left[ \frac{1.57 \pi I_y / I_{x_{1/2}} + 1}{2.25 \pi I_y / I_{x_{3/4}} + 1} \right] I_{x_{1/2}}}{I_{x_{3/4}}} \quad (33)$$



Since the upright should be stiffer than the ring, it was concluded that the relation  $I_u/I_r$  would be greater than one. This permitted the second terms in the denominator and numerator of the term in brackets in equation (33) to be neglected. Consequently, equation (33) simplified to the value;

$$\frac{\epsilon_{3/4}}{\epsilon_{1/2}} = \frac{2}{3} \quad (34)$$

Based on equation (34) a curved bar was chosen that described one-half a circle as the strained member of the load measuring device.

In order to combine algebraically, in correct relation for signs, the various strain gages were located on the curved bars at the two sections, A and B, in a Wheatstone Bridge circuit. Figure V. depicts a schematic model of the device and its' relative orientation. The arrows indicate the direction that the upright tips move when the slope of the elastic curve is positive. The sign convention employed for the strain remains positive for length change resulting from tension.



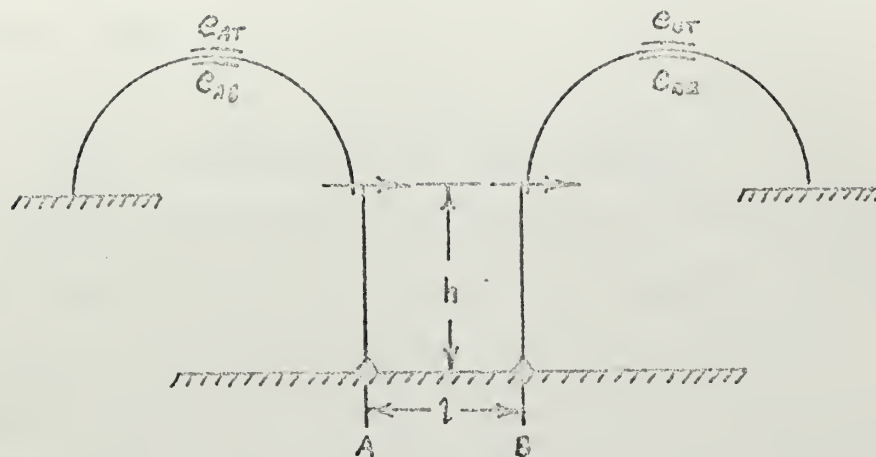


Figure V

Schematic Model Of Device Arrangement

Showing Strain Gage Placement

Based on equations (9), (21), and (31), the desired relation was

$$\tau_A + \tau_B \sim \epsilon_{measured} . \quad (35)$$

The relation of equation (35) was obtained by locating the strain gages in arms of the Wheatstone Bridge as shown in Figure VI.

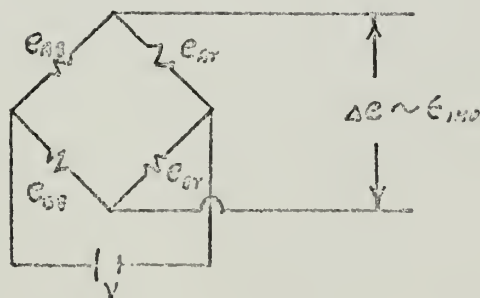


Figure VI.

Wheatstone Bridge Arrangement



The bridge arm's combined strains as shown in equation (36).

$$\epsilon_{ms} \sim [e_{as} - e_{ar} + e_{or} - e_{os}] \quad (36)$$

A check to determine maintenance of proper signs showed that if there was tension in  $e_{ar}$ , and compression in  $e_{os}$ , the indicated strain at the A section would be negative. This was correct since the tip movement required at A to produce the aforementioned state of strain would have to be to the left, referring to Figure V.. That tip movement could only result from negative elastic curve slope.





# RESULT

A portable load measuring device was conceptually formulated whose general schematic arrangement has been depicted in Figure V.. The functional relation of load to strain is

$$F = C_1 C_2 \epsilon_{measured} \quad (37)$$

where

$$C_1 = \text{constant} \times \frac{EI}{l^3}, \quad \text{constant} = \begin{cases} 6 - \text{cantilever} \\ 12 - \text{simple support} \end{cases} \quad (38)$$

and

$$C_2 = \frac{\pi}{2} \cdot \frac{R^2}{th} + \frac{1}{3} \cdot \frac{h^3}{R^2} \cdot \frac{E_r I_r}{E_s I_s} \quad (39)$$



DISCUSSION OF RESULTS

Analyzing a sample loading situation that the conceptually formulated device could be employed in revealed that the concept contains conflicting constants.<sup>1</sup> If the device were to be constructed to fit inside a hollow cylinder of expected dimensions, the moment of inertia of the curved bar member would have to exceed that of the upright by a very high value. This could be partially alleviated by selecting a material for the curved bar that had a Young's Modulus that was only a fraction of the modulus of the upright. However, any variation of modulus does not help the situation that the flexibility of the curved bar should only be one hundredth that of the upright, which is the reverse of one of the principle assumptions underlying the concept. By assuming the flexibilities were equal, the concept then required that the height of the devices upright be about ten times the radius of the thin curved bar. This would have dictated a curved bar of thickness approximately equal to five hundredths of an inch, which seems impractically tiny; or, the upright would have to be of such length that the device would no longer fit inside hollow cylinders of the size most likely to be encountered.

---

1. See APPENDIX IV



### CONCLUSIONS AND RECOMMENDATIONS

The concept of constructing a portable load measuring device based on a relation of elastic curve slope and induced strain is impractical due to the constraints on the device geometry.

Such a portable device would be of real value, and it is recommended that further study be made on the concept. A careful experimental analysis of the deformations of a hollow cylinder acting as a beam with varying end conditions should be a first step in further study.



APPENDIX





# APPENDIX I

## Manderla-Winkler Equations

The Manderla-Winkler Equations were derived by means of the moment area theorems,<sup>1</sup>. Assume that a portion of a beam has a  $M/EI$  curve as shown in Figure I, and an elastic curve as shown in Figure II. Utilizing the Second Moment Area Theorem, which states that the deflection of point 2 is equal to the  $M/EI$  curve between points 1 and 2 about an axis through point 1, the Manderla-Winkler Equations can be derived as follows:

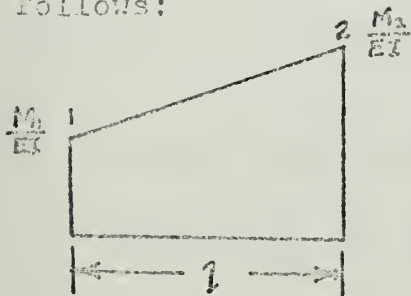


Figure A-I

$M/EI$  Curve

$$\tau_1 = \sin^{-1} \delta_2/l \cong \delta_2/l$$

$$-\tau_1 = \sin^{-1} \delta_1/l \cong \delta_1/l$$



Figure A-II

Elastic Curve

$$\text{assuming small slope} \quad (A-1)$$

$$\text{assuming small slope} \quad (A-2)$$

1. Norris, C.H. and Wilbur, J.B., Elementary Structural Analysis, -p.613



from 2<sup>nd</sup>. Moment Area Theorem

$$\delta_2 = \frac{M_1}{EI} (l)(l/2) + \frac{M_1 - M_2}{EI} (l/2)(l/3) = \frac{l^2}{6EI} [2M_1 + M_2] \quad (A-3)$$

from 2<sup>nd</sup>. Moment Area Theorem

$$\delta_1 = \frac{M_1}{EI} (l)(l/2) + \frac{M_1 - M_2}{EI} (l/2)(2l/3) = \frac{l^2}{6EI} [M_1 + 2M_2] \quad (A-4)$$

Substituting equations (A-3) and (A-4) into (A-1) and (A-2) and re-arranging

$$2M_1 + M_2 = \frac{6EI}{l} \tau_1 \quad (A-5)$$

$$M_1 + 2M_2 = -\frac{6EI}{l} \tau_2 \quad (A-6)$$

Solving (A-5) leads to the Manderla-Winkler Equations:

$$M_1 = M_{12} = \frac{2EI}{l} (2\tau_1 + \tau_2) \quad (A-7)$$

$$-M_2 = M_{21} = \frac{2EI}{l} (\tau_1 + 2\tau_2) \quad (A-8)$$

The Manderla-Winkler Equations utilize the following sign convention; slopes are positive when measured clockwise with reference to the chord connecting points 1 and 2, and moments are positive when clockwise on the end of the member. These equations are also valid only if there are no discontinuities in the  $M/EI$  curve within the portion under consideration.



APPENDIX II

Saint Venant's Principle<sup>1</sup>.

In both modeling and design, St. Venants' principle has been called upon. The principle states that: "If the loading on a small part of the boundry of an elastic system is replaced by a different loading, which is statically equivalent to the original loading, then the stress distribution in the system will be sensibly changed only in the neighborhood of the change; the stresses at a distance from the disturbance equal to the size of the disturbance itself will be changed by a few percent only." 2. St. Venants' principle is not a mathematical theorem or a law of nature, but is based on common sense and a large collection of mathematical and experimental results that bear out the principle.

An example of mathematical support of St. Venants' principle can be found in a study made of the stress distribution in a simply supported beam with a concentrated

---

1. First stated in St. Venants' memoir on torsion published in "Mem. Savants etrangers" Vol. 14, 1855.

2. Den Hartog, J.P., Advanced Strength of Materials, p. 117



load which was preformed by T.V. Karman and F. Seewald.<sup>1</sup>

Karman arrived at a stress function which gives the stress distribution in a beam when the bending moment diagram consists of a very narrow rectangle, as shown in Figure A-III.

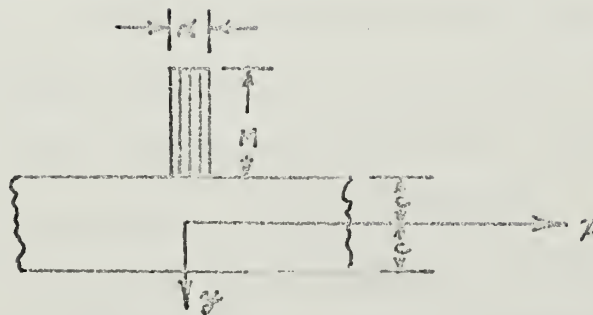


Figure A-III

Bending Moment Diagram

A stress function ( $\phi$ ) is a function of  $x$ ,  $y$  that is introduced to solve the equations of equilibrium and compstibility and to satisfy the boundary conditions.

$$\sigma_x = \frac{\partial^2 \phi}{\partial y^2} - \rho g y, \quad \sigma_y = \frac{\partial^2 \phi}{\partial x^2} - \rho g y, \quad \tau_{xy} = -\frac{\partial^2 \phi}{\partial x \partial y} \quad (A-9)$$

The stress function that Karman developed from consideration of Figure A-III was:

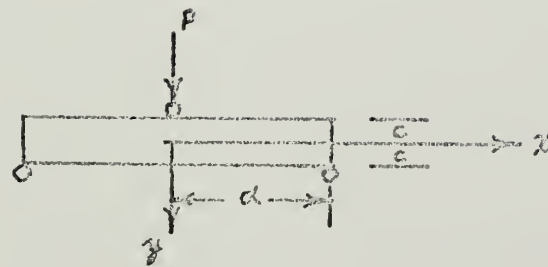
$$\begin{aligned} \phi = & \frac{Mc}{\pi} \int_0^{\infty} \frac{(\alpha c \cosh \alpha c + \sinh \alpha c) \cosh \alpha y - \sinh \alpha c \sinh \alpha y}{\sinh 2\alpha c + 2\alpha c} \cos \alpha x d\alpha \\ & - \frac{Mc}{\pi} \int_0^{\infty} \frac{(\alpha c \sinh \alpha c + \cosh \alpha c) \sinh \alpha y - \cosh \alpha c \cosh \alpha y}{\sinh 2\alpha c - 2\alpha c} \cos \alpha x d\alpha \end{aligned} \quad (A-10)$$

1. Timoshenko, S. and Goodier, J.N.; Theory of





Seewald utilized Karman's stress function to solve for the stress function of a beam subjected to a concentrated load. He did this by assuming that the bending moment diagram resulting from any loading could be broken up into small elements that would approach the rectangle used by Karman in developing equation (A-10). Seewald then integrated over the length of the beam to obtain a stress function appropriate to the simple beam with a concentrated load. He then divided the stress into two parts; the first part was calculated by application of the elementary beam formula, and the second part was termed  $\sigma_z'$  and represented by  $\beta(F/L)$  where  $\beta$  is a numerical factor that depends on position. Figure A-IV shows the results he obtained.



Simple Beam-Concentrated Load

Analyzed by Seewald

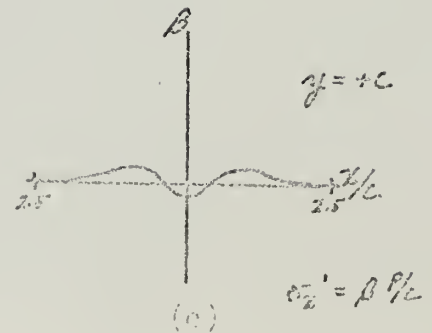
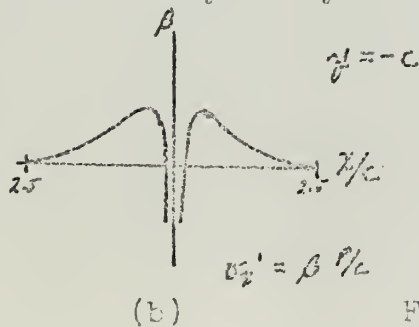


Figure A-IV

$\beta$  Determined By Seewald



The stress is the effect of local stresses arising near the point of load application which is superposed on the stress calculated using elementary beam formula. It is evident that in the most adverse position, in terms of applicability of simple theory for determining the stress distribution, the local effect of the load is negligible at distance greater than about 1.25 times the depth of the beam.



### APPENDIX III

#### CURVED BARS

The stress distribution and deflections of curved bars, cannot, in general, be analyzed using the theories that are applicable to initially straight elastic members. There are two approaches that can be taken; the first is to regard the bar as "thin", and the second is to regard it as "thick."

A bar in which the thickness,  $t$ , is 10 percent or less of the radius of curvature,  $R$ , is considered thin. In such a bar consider a small element,  $ds$ , that is the same order of magnitude as the thickness. The end sections of  $ds$  are not parallel to each other and since they are perpendicular to the curved center line they form an angle. However, this angle is of the same order of magnitude as  $t/R$  and can be neglected with the consequence that the ends are considered parallel. The inner and outer fibers of the element  $ds$  are also of different lengths, but once again this difference is neglected since the included angle between the end sections and the small  $t/R$  relation result in a small percentage difference in fiber lengths. The net effect is that the segment  $ds$  is regarded as substantially



straight, and straight beam theory is applied. To be specific, the neutral fiber passes through the center of gravity, the bending stress distribution is linear, the stress is given by equation (1) where  $y$  is the distance from the neutral axis to the point under consideration and the deformation is determined by equation (A-12) where  $d\theta$  is the change in angle that occurs in the angle between end sections  $ds$  apart when the segment  $ds$  is stressed.

$$\sigma = \frac{My}{I} \quad (A-11)$$

$$M = EI \frac{d\theta}{ds} \quad (A-12)$$

As an example, consider a cantilevered bar of arbitrary, (but  $t/R \gg 1$ ), curvature in one plane with a concentrated end load  $P$  at the free end as shown in Figure A-7.

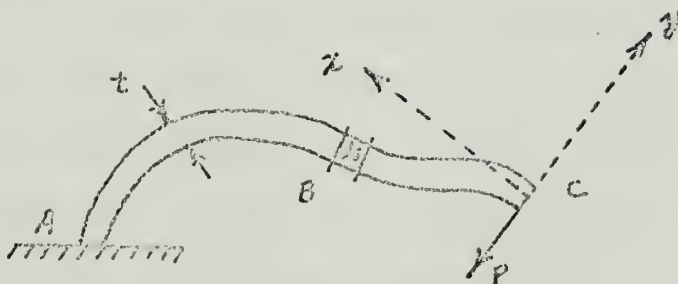


Figure A-7

Cantilevered Bar Of Arbitrary Curvature





By selecting the coordinate system so that the line of action of  $P$  is along one of the axis, the moment at any arbitrary point can be found by simply isolating the free end from the arbitrary point outward and multiplying  $P$  times the distance the line of force action is from the point. In the example shown in Figure A-V,  $M=Px$  and the stress is immediately determined using equation (A-12).

In determining the displacement of the free end some intuitive reasoning is necessary. In Figure A-V the segment  $ds$  is allowed to deform according to the moments exerted on it; however, the remainder of the bar is assumed to remain undeformed. This means that the section of bar from A to B is unaffected and that the section from B to C rotates as a rigid body through a small angle which causes angular deflection  $d\phi$ , displacement  $d\delta_y$ , along the line of load action and displacement  $d\delta_z$  in a direction perpendicular to the line of load action. In order to determine the total deflection at the free end one then merely takes the sum of all the small deflections caused by allowing small segments to flex by themselves from A to C.



From equation (2);

$$d\phi = \frac{M}{EI} ds \quad (A-13)$$

and from the geometry and assuming small angles;

$$d\delta_y = -x d\phi \quad (A-14)$$

$$d\delta_x = y d\phi \quad (A-15)$$

which after substituting (3) into (4) and (5), and integrating the equations for the movement of the free end become:

$$\phi = \int_s \frac{M}{EI} ds \quad (A-16)$$

$$\delta_x = \int_s \frac{My}{EI} ds \quad (A-17)$$

$$\delta_y = -\int_s \frac{Mx}{EI} ds \quad (A-18)$$

In cases when the curvature of the bar is sharp,  $t/R$  is greater than 10 percent, several of the factors that were neglected in the examination of thin bars can no longer be neglected. The principle factor that can no longer be ignored is the difference in length of the inner and outer fibers. The percentage difference has become significant, and this in turn makes assuming a linear distribution of tangential stress inaccurate. As the bar is deformed, the total deformation of the fibers is directly proportional to the distance of the fibers from the neutral surface; however, recalling that strain is deformation per unit length, one must note that the strains are not proportional to the distance from the



neutral surface due to the total length of the fibers. This means that within the elastic range ( $\sigma = E\epsilon$ ) of the material, the tangential stress is not linearly distributed.

Several approaches have been made in analyzing the stress distribution in thick curved bars, which includes the exact solutions,<sup>1</sup> least work solutions,<sup>2</sup> and hyperbolic solutions.<sup>3</sup> The hyperbolic, or Winkler-Bach, solutions have been related to the tangential stress distribution based on the simple beam formula by means of a constant.<sup>4</sup> The relation applies only to the outer and inner surface fibers and has been presented in tables for various cross sections and  $t/R$  ratios of bars that are subjected to bending only.

- 
1. Timoshenko, S. and Goodier, J.N. Theory of Elasticity, p.61-65 and p.73-78.
  2. Don Hartog, J.P. Advanced Strength of Materials, p.223-226
  3. Seely, F.B. and Smith, J.O. Advanced Mechanics of Materials, p.137-144
  4. Handbook of Engineering Fundamentals, edited by Pabback, O.W. p.5-39



The equation for use with the tables is:

$$\sigma_{\text{Circumferential}} = K \left( \frac{Mc}{I} \right) \quad (\text{A-19})$$

where

$$K = \frac{M}{AR} \left( 1 + \frac{1}{E} \cdot \frac{C}{R+C} \right) / \frac{Mc}{I} \quad (\text{A-20})$$

and M is the applied moment and is positive when decreasing the radius of curvature, C is the distance from the centroid axis to the fiber nearest the center of curvature, A is the cross sectional area, and R is the radius of curvature measured to the centroid axis, and  $\bar{x}$  is defined by equation (A-21).

$$\bar{x} = - \frac{1}{A} \int_A \frac{y}{R+y} dA \quad (\text{A-21})$$

In equation (A-21) y is measured from the centroidal axis and is positive when measured away from the center of curvature of the bar.

If in addition to a bending moment M, there is an axial load that passes through the centroid of the cross sectional area; the correction factor K is generally assumed to apply to the tangential stress due to axial load. The equation for the stress on an outer fiber under such a loading then becomes:

$$\sigma_{\text{circum.}} = K \left[ \frac{P}{A} + \frac{Mc}{I} \right] \quad (\text{A-22})$$





where P is taken as the axial load. Photoelastic analysis indicates that the maximum stress determined using equation (A-22) is quite close,<sup>1</sup>.

---

1. T.J. Dolan and R.L. Levin "A Study of the Stresses in Curved Beams" Proceedings of the Thirtieth Semi-Annual Eastern Photoelastic Conference, June, 1961.



# APPENDIX IV SAMPLE PROBLEM

In order to find out what scantings and size factors were involved an axle size and loading was assumed then analyzed to determine what such a loading meant in terms of strains and slopes. It was anticipated that the measuring device would be put inside the hollow cylinder; but, for purposes of the sample problem curved bar dimensions, upright dimensions, and etc., were chosen on the basis of approximate size limits rather than exact dimensions that would actually fit inside the assumed hollow cylinder.

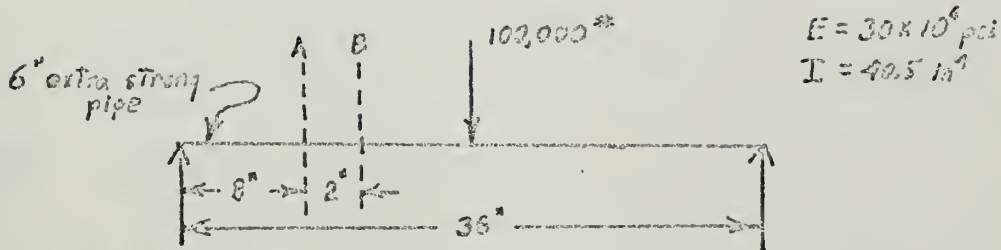


Figure A-VI

Assumed Loading

Calculations:

$$M_{AB} = (100,000) \left( \frac{8}{2} \right) = 400,000 \text{ in.-lb.} \quad (\text{A-23})$$

$$M_{BA} = -(100,000) \left( \frac{12}{2} \right) = -500,000 \text{ in.-lb.} \quad (\text{A-24})$$

$$2\tau_{AB} + \tau_B = \frac{1}{2EI} (M_{AB}) = \frac{400,000}{2EI} \quad (\text{A-25})$$

$$\tau_A + 2\tau_B = \frac{1}{2EI} (M_{BA}) = -\frac{500,000}{2EI} < -\frac{1}{2}$$



$$\frac{3}{2} \tau_n = \frac{650,000}{2EI} \quad (A-26)$$

$$\tau_n = 3.57 \times 10^{-4} \text{ radians}$$

$$\tau_c = \frac{400,000}{2EI} - \frac{1,300,000}{2EI} = -3.845 \times 10^{-4} \text{ rad.} \quad (A-27)$$

Assuming  $R=h$ ,  $R/t=10$ ,  $E_v = E_r$  :

$$C_2 = \left[ D \frac{R^2}{Et} + \frac{1}{3} \frac{h^2}{Rt} \frac{E_r I_r}{E_v I_v} \right] = 15.71 + 3.33 \frac{I_r}{I_v} \quad (A-28)$$

$$\tau_n = C_2 \epsilon_A \quad (A-29)$$

Assume minimum discernible value of  $\epsilon_A$  is  $1 \mu\text{strain}$

$$\text{required } \frac{I_r}{I_v} = \frac{1}{3.33} \left[ \frac{\tau_n}{\epsilon_A} - 15.71 \right] = 10.25 \quad (A-30)$$

Now assume  $E_r I_r / E_v I_v = 1$ ,  $R/t = 10$  :

$$C_2 = 5\pi \left( \frac{R}{h} \right) + \frac{10}{3} \left( \frac{h}{R} \right)^2 \quad (A-31)$$

$$C_2 = \frac{\tau_n}{\epsilon_A} = 357 \quad (A-32)$$

$$\left( \frac{h}{R} \right)^3 - 107 \left( \frac{h}{R} \right) + 17 = 0 \quad (A-33)$$

$$\text{required } \frac{h}{R} \cong 10 \quad (A-34)$$



BIBLIOGRAPHY

1. C.H. Norris and J.B. Wilbur; Elementary Structural Analysis; McGraw-Hill Book Co.; New York; 1960
2. S.H. Crandall and N.C. Dahl; An Introduction to the Mechanics of Solids; McGraw-Hill Book Co.; New York; 1959
3. J.P. Den Hartog; Strength of Materials; Dover Publications; New York; 1961
4. S. Timoshenko and J.N. Goodier; Theory of Elasticity; McGraw-Hill Book Co; New York; 1951
5. J.P. Den Hartog; Advanced Strength of Materials; McGraw-Hill Book Co.; New York; 1952
6. T.G. Peckwith; Mechanical Measurements;
7. F.B. Seely and J.O. Smith; Advanced Mechanics of Materials; Chapman and Hall Limited; London; 1952
8. S. Timoshenko; Theory of Plates and Shells; McGraw-Hill Book Co.; New York; 1940
9. M. Hetenyi; Handbook of Experimental Stress Analysis; John Wiley and Sons, Inc.; New York; 1950
10. O.W. Fishbach; Handbook of Engineering Fundamentals; John and Wiley and Sons, Inc.; New York; 1961
11. T.N. Whitehead; The Design and Use of Instruments and Accurate Mechanism; The Macmillan Co.; New York; 1934





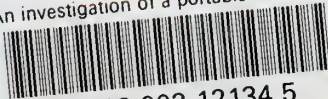
12. S. Timoshenko; Theory of Elastic Stability;  
McGraw-Hill Book Co.; New York; 1936
13. A.C. Ruge and F.O. Schmidt; "Mechanical Structural  
Analysis by the Moment Indicator;" Proceedings of  
American Society of Civil Engineers; October, 1938
14. G.K. Ozolins; "An Investigation of the Stress  
Distribution and Deformation of Cylindrical Shell  
due to Concentrated Loads"  
M.I.T. Mechanical Engineering Department Thesis; 1961
15. E.B. Debbas; "Relations of Curvature Changes to  
Deflections in Curved Elements;"  
M.I.T. Civil Engineering Department Thesis; 1961





thesK3893

An investigation of a portable device fo



3 2768 002 12134 5

DUDLEY KNOX LIBRARY